Fat-Saturation MR Imaging of the Upper Abdomen

Richard C. Semelka[1]
Wilbert Chew
Hedvig Hricak
Ernesto Tomei
Charles B. Higgins

The fat-saturation (fatsat) MR technique decreases the signal intensity of fat, thereby enhancing the definition of upper abdominal organs and reducing artifacts while maintaining the T1 and T2 information available on spin-echo sequences. To evaluate the potential of fatsat in examining the abdomen, we conducted a prospective study involving 30 subjects, including four normal volunteers, 18 patients investigated for liver disease, and eight patients studied for miscellaneous abdominal disease. Short TR, 300–600/15–20 (TR/TE), and long TR, 2000–2500/20–30, 70–80, spin-echo images with and without fatsat were compared. The images were evaluated both qualitatively and quantitatively. Qualitative assessment was made with receiver-operating-characteristic (ROC) curve analysis of the confidence level of observers to detect the presence of disease, comparing fatsat with standard spin-echo sequences. ROC analysis showed greater interpreter confidence and accuracy for fatsat sequences than for standard spin-echo sequences. The measured signal-difference-to-noise (SD/N) ratio comparing upper abdominal organs with surrounding tissue revealed the highest values for short TR/TE regular spin echo, followed by short TR/TE fatsat. The highest SD/N ratio for hepatic masses was with long TR/TE fatsat followed by short TR/TE fatsat.

The results of this study suggest that the fatsat technique may improve abdominal MR imaging.

***AJR* 155:1111–1116, November 1990**

Techniques have been devised to enhance contrast between diseased and normal tissue by attenuation of the signal from fat [1–13]. The fat-saturation (fatsat) technique suppresses the signal of fat by transmitting a low-amplitude, long-duration RF pulse centered on the frequency of lipid resonance followed by a gradient pulse to disperse this signal. A spin-echo sequence is then performed with signal reception centered on the frequency of water. T1 and T2 information is unaffected by this procedure, and therefore the specificity this information provides is not lost, unlike with short-T1 inversion recovery (STIR) [4, 5]. A disadvantage of the STIR sequence is substantial loss of signal intensity [4, 5]. This problem may not exist with the fatsat spin-echo technique. Reduction of fat signal intensity in the abdomen can be important because (1) the bright signal intensity of fat caused by cardiac and respiratory motion induces phase artifacts, degrading image quality [5], and (2) fat creates chemical-shift artifacts [14], which are particularly problematic for evaluation of the renal cortex. Fatsat MR imaging can be applied for short TR and long TR spin-echo sequences. Especially at high field strength, long TR/TE images have been effective and necessary for detection of hepatic lesions [15, 16].

To evaluate the potential of fatsat for MR imaging of the abdomen, we compared short and long TR sequences with fatsat and conventional spin echo in normal subjects and patients with abdominal disease, with qualitative assessment described by receiver-operating-characteristic (ROC) curve analysis and by measurement of signal-difference-to-noise (SD/N) ratios.

Received March 9, 1990; accepted after revision May 30, 1990.

[1] All authors: Department of Radiology, Box 0628, University of California Medical School, San Francisco, CA 94143. Address reprint requests to C. B. Higgins.

0361-803X/90/1555-1111

Subjects and Methods

Patients

Thirty subjects were studied in a consecutive series, including four normal subjects, 18 patients investigated for liver disease (three with hepatocellular carcinoma, two with other primary malignant tumors, six with metastases, one with a hepatic hemangioma, three with cirrhosis, one with hepatic fibrosis, and two with masses of unknown cause), and eight patients with miscellaneous abdominal disease (two with malignant tumors, three with benign retroperitoneal fibrosis, one with benign renal calcifications, and two with no abnormalities). The study population included 18 men and 12 women 8–71 years old (mean, 54 years). Excluding the normal volunteers, correlation with other imaging studies was available for all patients, including CT within 1 month of the MR study (n = 24), sonography within 1 month of the MR study (patient with hepatic fibrosis), and serial CT and MR studies every 3–6 months for 3 years (one patient with metastases). MR findings were correlated with pathologic findings from surgery (n = 11) or biopsy (n = 5).

MR Imaging

Imaging was performed on a 1.5-T cryogenic magnet (Signa, General Electric, Milwaukee, WI). Short TR, 300–600/15–20 (TR/TE), and long TR, 2000–2500/20,70–80, spin-echo images were obtained, both with (n = 30, short TR; n = 11, long TR) and without (n = 30, short and long TR) fatsat. Long TR fatsat sequences were not acquired in the initial 19 subjects in this study. As implementation of the fatsat technique results in loss of approximately 15% of the slices obtained by regular spin echo when using the same TRs and TEs, slight variations (never exceeding 25%) in these parameters were necessary with fatsat in order to ensure the same coverage. Images of the abdomen were acquired in the axial plane. Respiratory compensation and superior and inferior saturation pulses were used in all studies. Matrix size was 256 × 192 with two excitations in all studies. Slice thickness and interslice gap were kept constant between all sequences in the same study (5- to 10-mm gap). Fatsat sequences were performed after regular spin-echo sequences.

Fatsat Technique

Fatsat was performed by transmitting a chemically selective RF pulse centered on the frequency of lipid resonance with subsequent dispersion of the signal with a slice-selective gradient pulse. The spin-echo sequence was then performed with signal reception centered on the frequency of water (Fig. 1).

Image Analysis

ROC analysis was performed by three independent radiologists. The various image sequences were randomly sorted and interpreted in a blinded fashion. Information provided by short TR and long TR sequences for regular spin echo was considered one information set and was compared with fatsat sequences, either short TR alone, or in combination with long TR in 11 cases. Short and long TR images were interpreted together in order to evaluate whether fatsat could substitute for spin echo in the clinical setting. Five categories of confidence were used: (1) definitely negative, (2) probably negative, (3) possibly positive, (4) probably positive, and (5) definitely positive. The presence of disease was evaluated. Determination of true presence was made on the basis of pathologic findings from surgery (n = 11) or biopsy (n = 5). When pathologic findings were not available, the maximum information from all imaging studies was treated as true presence of disease (n = 10). True-positive and false-positive fractions were calculated, comparing confidence of interpretation with true presence [17].

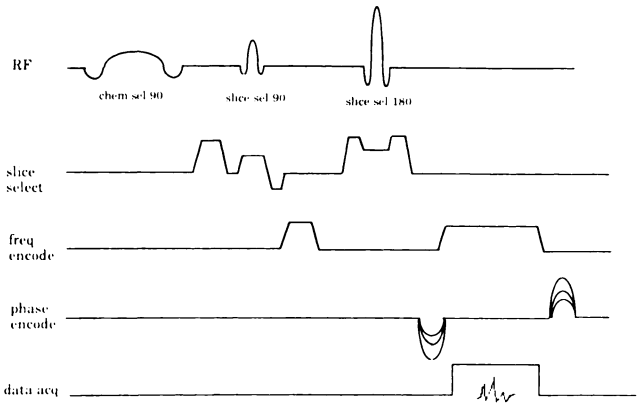

Fig. 1.—Pulse sequence for the fat-saturation spin-echo pulse sequence. chem = chemically, sel = select, freq = frequency, acq = acquisition.

An attempt was made to semiquantify the interpreters' overall impression of organ architecture in order to evaluate subjective information in a systematic way. To achieve this, definition of organ morphology was analyzed by three independent radiologists, concurrent with the ROC analysis. The ability to define internal structures and detect edges of normal organs and abnormalities was rated on the following scale: 0 = not visible, 1 = possibly visible, 2 = definitely visible, and 3 = easily visible and sharply defined. For individual organs, specific detail was assessed: for the liver, edge delineation; for the biliary tree and intrahepatic vasculature, sharpness; for the spleen, sharpness of the edge and hilar vasculature; for the pancreas, visualization of the uncinate process, head, body, tail, pancreatic duct in the body and tail, and common bile duct in the head of the pancreas; for the adrenal glands, visualization of both limbs and body (mean value for both glands); for the kidneys, corticomedullary differentiation and sharpness of renal outline.

Quantitative assessment of signal intensity was obtained by operator-defined regions of interest (ROIs). Data were expressed as the SD/N ratio of organs to surrounding tissue. The image display adds 1024 to pixel signal intensity and, therefore, this number was subtracted from all ROI determinations. Noise was measured by a large rectangular ROI anterior to the abdomen. The standard deviation of noise was used for calculations of SD/N. Liver, spleen, pancreas, and adrenal glands were compared with retroperitoneal fat; renal cortex was compared with medulla; liver lesions were compared with surrounding liver; and upper abdominal abnormalities were compared with retroperitoneal fat.

Statistical Analysis

All SD/N measurements and morphologic detail ratings were calculated as mean values ± standard deviation. Scheffe's test for multiple comparisons was applied to detect differences by multivariate analysis.

Results

ROC analysis by three independent radiologists comparing standard spin-echo and fatsat sequences showed a greater

degree of confidence with fatsat in detecting the presence of disease. The higher confidence level is demonstrated by the position of the curve for the fatsat sequence compared with the curve for the regular spin-echo sequence (Fig. 2). A moderate statistical difference ($p < .05$) was present between the curves.

Table 1 contains SD/N data for short TR/TE, long TR/short TE, and long TR/TE sequences with and without fatsat. SD/N was greatest in short TR/TE regular spin-echo sequences for liver, spleen, pancreas, and adrenal glands, followed by long TR/short TE fatsat and short TR/TE fatsat. The values on regular short TR/TE images were negative because of the very bright signal intensity from fat. These values were all positive with the fatsat technique because the upper abdominal organs were higher in signal intensity than retroperitoneal fat was. Measured SD/N values for hepatic lesions were significantly higher for long TR/TE fatsat ($p < .01$) and moderately higher for short TR/TE fatsat ($p = .05$) than for all regular spin-echo sequences. No other statistically significant differences were observed between imaging sequences.

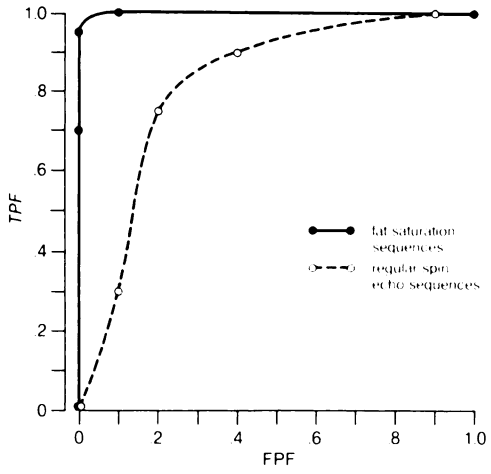

Fig. 2.—Receiver-operating-characteristic curve analysis for the presence of disease ($n = 30$). TPF = true-positive fraction, FPF = false-positive fraction.

Figure 3 illustrates the appearance of abdominal organs on images obtained by using the fatsat technique with short TR/TE and with long TR/TE sequences; the same levels were studied with regular spin-echo images for comparison. Compared with standard spin echo, images with fatsat showed improved delineation of the margins and internal morphology of liver, spleen, pancreas, adrenal glands, and kidneys. Improved definition of the abdominal organs is apparent owing to the relatively high signal intensity of these organs in the background of suppressed retroperitoneal fat.

In addition to the relative brightening of organs, the degree of noise was greatly diminished. Noise from respiratory and cardiac activity was greatly diminished, which permitted better visualization of the left lobe of the liver (Fig. 4). Fatsat sequences were more sensitive to lesion detection. In three of the five patients with hepatic metastases, long TR/TE fatsat permitted visualization of lesions not apparent on non-fat-suppressed sequences (51 vs 36 lesions) (Fig. 5).

The ability to define internal organ morphology was rated superior (27/30) and equivalent (3/30) when comparing fatsat and regular spin echo. Table 2 gives the data expressed as individual organs and hepatic disease. The subjective rating of the depiction of the pancreas and adrenal glands on short TR and long TR images and corticomedullary difference on short TR images was statistically superior ($p < .01$) for fatsat images compared with regular spin-echo images.

Fatsat was more specific in two of five cases of primary malignant tumor, by demonstrating sparing of the lateral segment of the left lobe, which was not evident on the standard spin-echo images.

On fatsat images, the signal intensity of fat was lowered to a level comparable to that of fibrous tissue, so that the contrast between the two was lessened. Fatsat showed diminished contrast between fibrous tissue and fat in patients with benign retroperitoneal fibrosis ($n = 3$), while standard spin-echo images showed clearly the presence of disease because of higher contrast.

Discussion

Various techniques are used to increase the signal difference between diseased tissue and surrounding structures

TABLE 1: Signal-Difference-to-Noise Ratios for Abdominal Organs and Liver Lesions

Region	Short TR/Short TE		Long TR/Short TE		Long TR/Long TE	
	Without Fatsat ($n = 30$)	With Fatsat ($n = 30$)	Without Fatsat ($n = 30$)	With Fatsat ($n = 11$)	Without Fatsat ($n = 30$)	With Fatsat ($n = 11$)
Liver	−19.4 ± 9.1	11.9 ± 4.8	−14.9 ± 5.0	11.3 ± 3.9	−8.6 ± 4.0	4.6 ± 5.1
Spleen	−23.2 ± 9.4	9.1 ± 4.4	−12.0 ± 4.9	12.2 ± 4.9	−4.2 ± 4.7	9.1 ± 6.4
Adrenal, fat	−19.3 ± 11.5	10.5 ± 4.0	−12.1 ± 4.5	11.8 ± 4.5	−4.9 ± 3.8	7.2 ± 4.0
Pancreas, fat	−19.5 ± 9.0	12.7 ± 5.7	−10.9 ± 4.8	15.4 ± 5.7	−4.9 ± 4.8	6.5 ± 1.7
Renal corticomedullary boundary	3.1 ± 2.0	7.7 ± 2.9	1.7 ± 1.4	5.0 ± 3.5	1.4 ± 0.9	3.2 ± 2.1
Lesion, liver	−3.8 ± 2.3	−7.3 ± 5.0[a]	1.3 ± 3.1	2.2 ± 3.8	4.2 ± 1.9	12.6 ± 3.1[b]

Note.—Values are means ± SD. Fatsat = fat saturation.

[a] Moderately significant ($p < .05$).

[b] Statistically significant ($p < .01$).

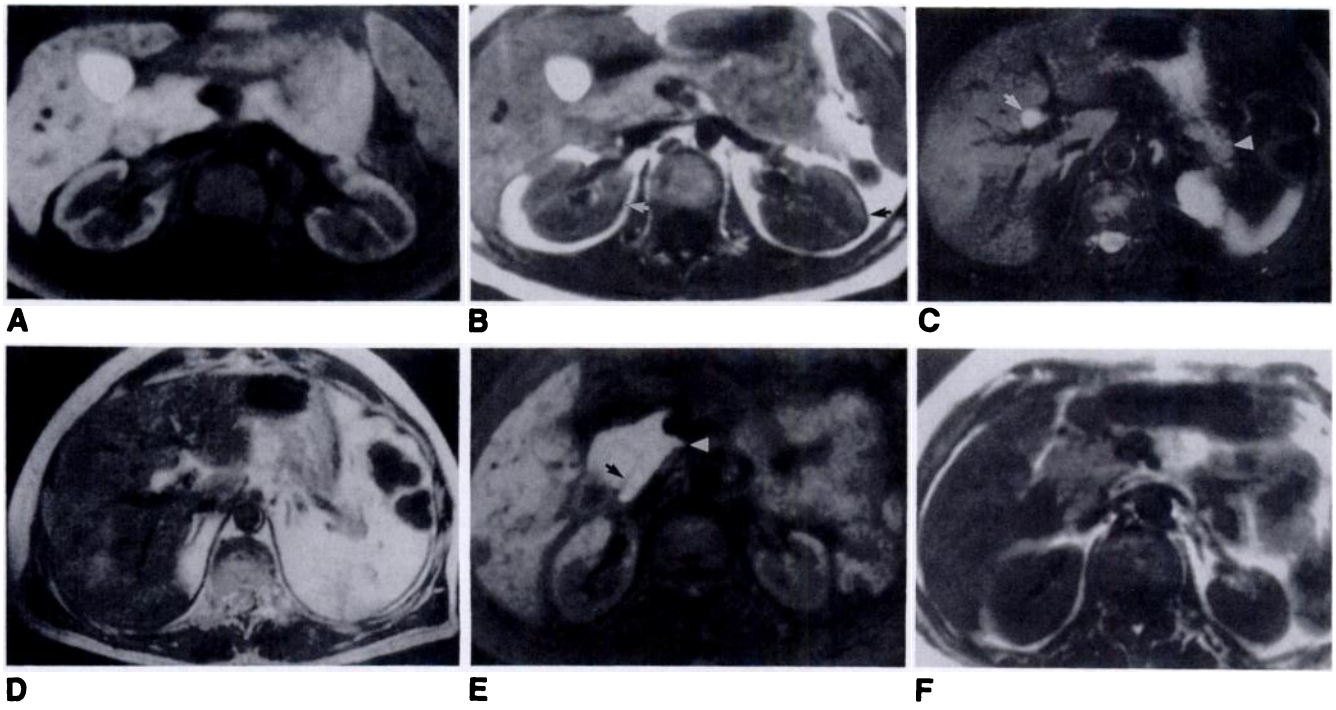

Fig. 3.—Images illustrating appearance of organs with and without fat saturation (fatsat).

***A* and *B*, Short TR/TE (600/20) fatsat (*A*) and regular spin-echo (*B*) images of normal kidneys. Improved corticomedullary differentiation and absence of chemical-shift artifact are apparent on fatsat image (*arrows* point to chemical-shift artifact on regular spin-echo image).**

***C* and *D*, Long TR/TE (2000/70) fatsat (*C*) and regular spin-echo (*D*) images of normal adrenal glands in a patient with hepatic metastases from colonic cancer. Adrenal glands are better depicted and common hepatic duct (*arrow*) is sharply defined and separated from fat in the porta hepatis with fatsat technique. In addition, lobulations of pancreatic tail are apparent on fatsat image (*arrowhead*), but not on regular spin-echo image.**

***E* and *F*, Short TR/TE (300/20) fatsat (*E*) and regular spin-echo (*F*) image of normal head of pancreas in a patient with gastrinoma metastatic to liver. Head of pancreas is relatively brighter than all surrounding tissue on fatsat compared with regular spin-echo image; common bile duct (*arrow*) is better delineated as it enters duodenum, and uncinate process is sharper in outline (*arrowhead*). Note also that hepatic metastases are better depicted with fatsat.**

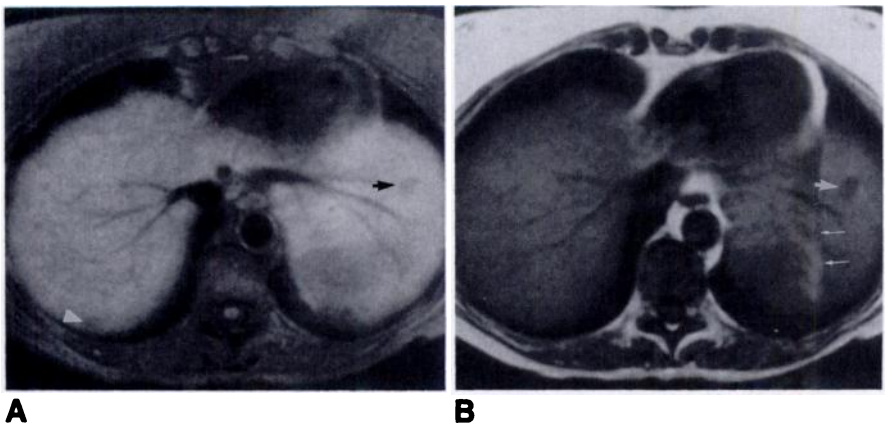

Fig. 4.—Patient with liver masses of unknown cause.

***A* and *B*, Short TR/TE (400/15) fat-saturation (fatsat, *A*) and short TR/TE (300/20) regular spin-echo (*B*) images. Fatsat image has less artifact from cardiac activity than does regular spin-echo image (*long arrows*), permitting improved visibility of left lobe of liver. Liver vasculature is more sharply defined. Low-intensity mass is apparent on both images (*short arrows*); a second lesion in posterior segment of right lobe on fatsat image (*arrowhead*) was not seen on short TR/TE regular spin-echo image, but was identified on TR/TE regular spin-echo image (*not shown*).**

and hence the depiction of abnormalities by suppressing the high signal intensity of fat. Examples of fat-suppression techniques are the Dixon method [8–10], STIR [1–5], chopper fat suppression [6, 7], and chemical shift–selective (CHESS) imaging [11]. These techniques have been used in various anatomic sites where fat is a prevalent background tissue, and the suppression of fat permits better evaluation of disease. Fat suppression is useful in the upper abdomen because the motion of high-signal-intensity fat degrades image quality by inducing phase artifacts [5]. This can be diminished by fat-suppression techniques.

Fatsat is a modification of the spin-echo technique and therefore has the T1 and T2 information of regular spin-echo imaging. The specificity of lesion characterization provided by this information is maintained. With the STIR technique, there is signal addition of T1 and T2 information, which, among other things, renders the differentiation of tumor from edema difficult [5].

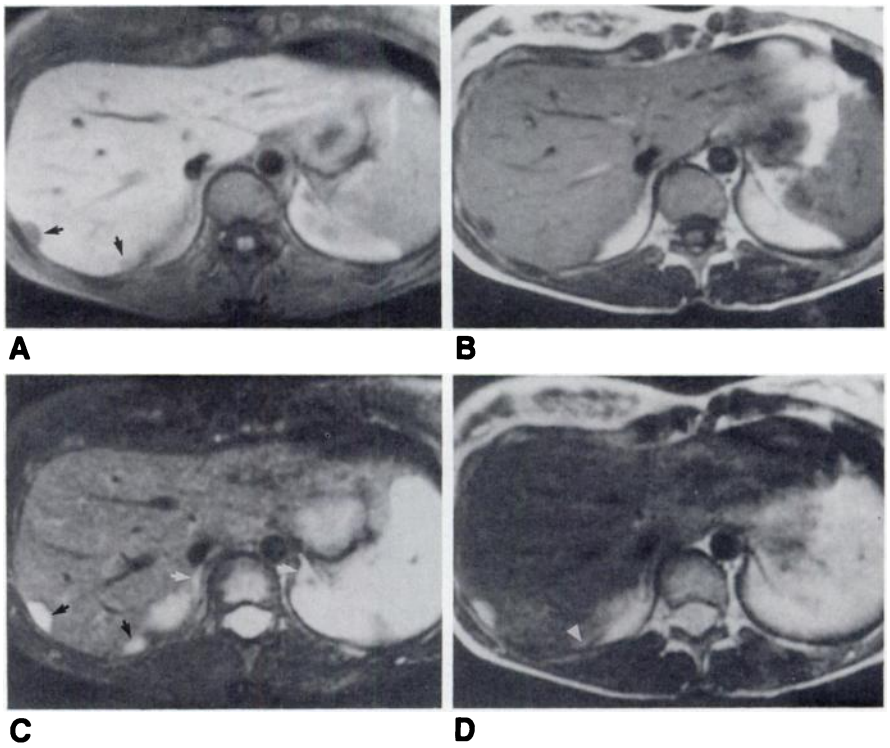

Fig. 5.—Patient with breast cancer metastatic to liver.

***A–D*, Short TR/TE (300/20) fat-saturation (fatsat, *A*) and regular spin-echo (*B*) and long TR/TE (2000/70) fatsat (*C*) and regular spin-echo (*D*) images. Two subcapsular metastatic deposits are well depicted on short and long TR fatsat images (*black arrows*), while on regular spin-echo images only one lesion was identified prospectively. Second lesion is apparent in retrospect on long TR/TE regular spin-echo image (*arrowhead*). Note high signal intensity of adrenal glands on long TR/TE fatsat image, providing excellent delineation from surrounding tissue (*white arrows*).**

TABLE 2: Definition of Morphology of Normal Organs and Liver Lesions

Region	Short TR/Short TE		Long TR/Short TE		Long TR/Long TE	
	Without Fatsat (n = 30)	With Fatsat (n = 30)	Without Fatsat (n = 30)	With Fatsat (n = 11)	Without Fatsat (n = 30)	With Fatsat (n = 11)
Liver	2.3 ± 0.08	2.9 ± 0.06	2.0 ± 0.06	2.7 ± 0.07	1.7 ± 1.0	2.2 ± 0.08
Spleen	2.3 ± 0.08	2.4 ± 0.07	2.3 ± 0.08	2.4 ± 0.07	1.7 ± 1.0	2.3 ± 0.07
Adrenals	2.0 ± 0.06	2.9 ± 0.03[a]	2.0 ± 0.06	2.9 ± 0.03[a]	1.3 ± 1.0	2.3 ± 0.08[a]
Pancreas	1.8 ± 0.07	2.8 ± 0.04[a]	1.8 ± 0.07	2.9 ± 0.04[a]	1.3 ± 1.0	2.2 ± 0.08[a]
Renal cortico-medullary boundary	1.8 ± 0.07	2.4 ± 0.07[a]	0.4 ± 0.08	2.2 ± 0.08[a]	0.4 ± 0.08	1.6 ± 0.08
Liver disease	2.1 ± 0.08	2.7 ± 0.07[a]	0.6 ± 0.06	1.6 ± 1.0	2.2 ± 1.0	2.8 ± 1.2

Note.—Values are means ± SD. Internal morphology was rated on a scale of 0–3: 0 = not visible; 1 = possibly visible; 2 = definitely visible; 3 = easily visible, sharply defined. Fatsat = fat saturation.

[a] Statistically significant difference ($p < .01$).

The elimination of chemical-shift artifacts minimizes loss of anatomic detail around the edges of structures surrounded by fat [14]. The ability to visualize sharp margins of all abdominal organs with fatsat is to a large extent due to the removal of the chemical-shift artifact.

No postprocessing is required with fatsat, which is an advantage over other techniques [8–10]. However, approximately 15% of the slices are lost compared with regular spin echo with the same parameters, because of the time required to transmit the chemically selective pulse.

ROC analysis showed that greater confidence in evaluating disease was provided with fatsat than with standard spin echo, and fatsat was also better able to define organ morphology for the liver, pancreas, kidneys, and adrenal glands. This superior performance probably was due to three factors: (1) With fatsat phase artifacts are diminished and chemical-shift artifacts are absent, providing sharper depiction of organ architecture compared with regular spin echo. (2) With standard spin echo, other structures such as vessels, bowel, muscle, and fibrous tissue are also low in signal intensity, so that they can be difficult to distinguish from organs (particularly adrenal glands and pancreas), while with fatsat solid organs appear relatively bright and these other structures have lower signal intensity (see Fig. 3). Fatsat reduces the dynamic range of signal intensities in the abdomen, thereby expanding the signal intensity range between organs and nearby bowel and fibrous and vascular tissue, rendering the organs relatively bright in signal intensity. (3) Structures are

more easily defined when they are of high intensity in a dark background rather than the reverse.

Fatsat sequences were useful in evaluating liver disease, increasing both sensitivity and specificity. In patients with hepatic metastases, greater confidence in detection was demonstrated with fatsat, in one of five, and fatsat identified more lesions in three of five cases. Improved specificity was shown in the ROC analysis, in which fatsat showed high confidence in sparing of the lateral segment in two cases of primary malignant tumor, while standard spin echo showed low confidence. In both cases, pathologic examination confirmed sparing of the lateral segment. The ability to define the extent of involvement (e.g., if segments are spared and the tumor is therefore resectable), is an important determination. The quantitative data for hepatic masses showed the highest values for long TR/TE fatsat, followed by short TR/TE fatsat (see Table 2). Comparable results at mid-field strength have been reported recently using the Dixon method of fat attenuation [10].

One drawback of fatsat is that contrast between fat, muscle, and fibrous tissue is lessened on all sequences. Therefore, if the disease is fibrous in nature, it may be less conspicuous with fatsat than with regular spin echo. This was the case for the patients with benign retroperitoneal fibrosis in our study. However, despite decreased contrast, the extent of disease may be better appreciated with fatsat.

The difficulties with fatsat are (1) the technical requirement of identification of the spectral peak of lipids on which to center the chemically selective pulse; (2) the slight inhomogeneity of the fat suppression at the periphery of the image and at the levels farthest from the central slice of an acquisition series, because the local resonant frequency of fat at these locations is slightly different from the chemically selective pulse [13]; and (3) that 15% fewer slices are obtained than with standard spin-echo sequences.

Although the results of this study are encouraging, this technique was not compared with other fat-attenuating sequences and pathologic proof was not available for all patients. Further evaluation in a larger prospective series is warranted before the role of fatsat in MR imaging is determined.

REFERENCES

1. Paling MR, Abbitt PL, Mugler JP, Brookeman JR. Liver metastases: optimization of MR imaging pulse sequences at 1.0 T. *Radiology* **1988**;167:695–699
2. Bydder GM, Steiner GM, Blumgart LH, Khenia S, Young IR. MR imaging of the liver using short T1 inversion recovery sequences. *J Comput Assist Tomogr* **1985**;9:1084–1089
3. Atlas SW, Grossman RI, Hackney DP, Goldberg HI, Bilaniuk LT, Zimmerman RA. STIR MR imaging of the orbit. *AJNR* **1988**;9:969–974
4. Bydder GM, Young IR. MR imaging: clinical use of the inversion recovery sequence. *J Comput Assist Tomogr* **1985**;9:659–675
5. Shuman WP, Baron RL, Peters MJ, Tanzioli PK. Comparison of STIR and spin-echo MR imaging at 1.5 T in 90 lesions of the chest, liver, and pelvis. *AJR* **1989**;152:853–859
6. Simon J, Szumowski J, Totterman S, et al. Fat suppression MR imaging of the orbit. *AJNR* **1988**;9:961–968
7. Szumowski J, Plewes DB. Separation of lipid and water MR imaging signals by chopper averaging in the time domain. *Radiology* **1987**;165: 247–250
8. Lee JKT, Heiken JP, Dixon WT. Detection of hepatic metastases by proton spectroscopic imaging. *Radiology* **1985**;156:429–433
9. Scherty LD, Lee JKT, Heiken JP, Molina PL, Totty WG. Proton spectroscopic imaging (Dixon method) of the liver: clinical utility. *Radiology* **1989**;173:401–405
10. Rummeny E, Saini S, Stark DD, Weissleder R, Compton CC, Ferrucci JT. Detection of hepatic metastases with MR imaging: spin-echo vs phase-contrast pulse sequences at 0.6 T. *AJR* **1989**;153:1207–1211
11. Frahm J, Haase A, Hanicke W, Matthaei D, Bomsdorf H, Helzel T. Chemical shift selective MR imaging using a whole-body magnet. *Radiology* **1985**;156:441–444
12. Keller PJ, Hunter WW, Schmalbrock P. Multisection fat-water imaging with chemical shift selective presaturation. *Radiology* **1987**;164:539–541
13. Mitchell DG, Vinitski S, Rifkin MD, Burk DL Jr. Sampling bandwidth and fat suppression: effects on long TR/TE MR imaging of the abdomen and pelvis at 1.5 T. *AJR* **1989**;153:419–425
14. Daniels DL, Kneeland JB, Shimakawa AJ, et al. MR imaging of the optic nerve and sheath: correcting the chemical shift misregistration effect. *AJNR* **1986**;7:249–253
15. Foley WD, Kneeland JB, Cates JD, et al. Contrast optimization for the detection of focal hepatic lesions by MR imaging at 1.5 T. *AJR* **1987**; 149:1155–1160
16. Marchal G, van Hecke P, Demaerel P, et al. Detection of liver metastases with superparamagnetic iron oxide in 15 patients: results of MR imaging at 1.5 T. *AJR* **1989**;152:771–775
17. Metz CE. Basic principles of ROC analysis. *Semin Nucl Med* **1978**;8: 283–298